HAL
open science

A note on model reduction for microelectromechanical systems

Joachim Escher,, Pierre Gosselet, Christina Lienstromberg

To cite this version:

Joachim Escher,, Pierre Gosselet, Christina Lienstromberg. A note on model reduction for microelectromechanical systems. Nonlinearity, 2017, 30 (2), pp.454-465. 10.1088/1361-6544/aa4ff9 . hal-01421893

HAL Id: hal-01421893

https://hal.science/hal-01421893

Submitted on 6 May 2021

HAL is a multi-disciplinary open access archive for the deposit and dissemination of scientific research documents, whether they are published or not. The documents may come from teaching and research institutions in France or abroad, or from public or private research centers.

L'archive ouverte pluridisciplinaire **HAL**, est destinée au dépôt et à la diffusion de documents scientifiques de niveau recherche, publiés ou non, émanant des établissements d'enseignement et de recherche français ou étrangers, des laboratoires publics ou privés.

A note on model reduction for microelectromechanical systems

Joachim Escher[1], Pierre Gosselet[2] and Christina Lienstromberg[1,2]
(1) Institut für Angewandte Mathematik,
Leibniz Universität Hannover, Hannover, Germany
(2) LMT-Cachan/ENS-Cachan, CNRS, Université Paris-Saclay, France
E-mail: escher@ifam.uni-hannover.de, lienstromberg@ifam.uni-hannover.de,
pierre.gosselet@ens-paris-saclay.fr

May 6, 2021

Abstract

Numerical evidence is provided that there are non-constant permittivity profiles which force solutions to a two-dimensional coupled moving boundary problem modelling microelectromechanical systems to be positive, while the corresponding small-aspect ratio model produces solutions which are always non-positive.

Keywords: MEMS, free boundary value problem, general permittivity profile, small-aspect ratio limit

Mathematics Subject Classification numbers: 35R35, 35B09, 35B44, 74M05

1 Introduction

In this note we report on some recent investigations of qualitative properties of solutions to microelectromechanical systems (MEMS) with general permittivity. Idealised MEMS devices consist of two key components: a rigid ground plate and a thin dielectric elastic membrane that is suspended above the ground plate and fixed along its boundary. In practice the mem- brane's upper surface is often coated with a thin conducting film. By applying a given voltage to the conducting film, such that the ground plate and the membrane are at different electric potentials, a Coulomb force is induced across the device. The transformation of electrostatic energy into mechanical energy in turn causes a deformation of the membrane, see figure **??**. Mathematical models have been set up to predict the evolution of such MEMS in which the state of the device is fully described by the deformation u of the membrane and the electrostatic potential ψ. In order to describe the system precisely, let $I := (1,1)$ denote the dimensionless horizontal length of the device and let $f = f(x)$ denote a smooth[1] and positive permittivity profile defined on $[-1,1]$. Finally, we assume that there is no variation of both, u and ψ in the y-direction, i.e. the horizontal direction orthogonal to the x-direction. Then we consider the coupled system consisting of the semilinear parabolic initial boundary value problem

$$u_t - u_{xx} = -\lambda\left(\varepsilon^2\psi_x^2(t,x,u) + \psi_z^2(t,x,u)\right) + 2\lambda\varepsilon\Psi_x(t,x,u), \quad t>0,\ x\in I, \tag{1}$$

$$u(t,\pm 1) = 0, \quad t>0, \tag{2}$$

$$u(0,x) = u_*(x), \quad x\in I \tag{3}$$

describing the time evolution of the displacement $u = u(t,x)$ of the membrane, whereas the electrostatic potential $\psi = \psi(t,x,z)$ is given as the solution to the rescaled elliptic free boundary value problem

$$\varepsilon^2\psi_{xx} + \psi_{zz} = 0, \quad t>0,\ (x,z)\in\Omega(u(t)), \tag{4}$$

$$\psi(t,x,z) = \frac{1+z}{1+u(t,x)}f(x), \quad t>0,\ (x,z)\in\partial\Omega(u(t)). \tag{5}$$

In the above system $\varepsilon > 0$ denotes the aspect ratio of the unscaled device, i.e. the ratio of the undeformed gap size to the length of the device. Recall that the aspect ratio ε, appearing in particular in (4), is a positive constant, expressing the fact that the nominal gap of the device is not negligible. This means that we do not ignore effects due to fringing fields. However, we consider a membrane of vanishing thickness and describe dielectric properties[2] of it by the so- called permittivity profile $f = f(x),\ x\in I$, appearing

[1] Smoothness is assumed solely for simplicity, see theorem 1.1

[2] We assume the elastic plate / membrane to be of infinitesimal thickness, whence its dielectric properties are summarised in the function $f = f(x)$. The introduction of the profile $f = f(x)$ is also suitable to model piezoelectric effects of the membrane.

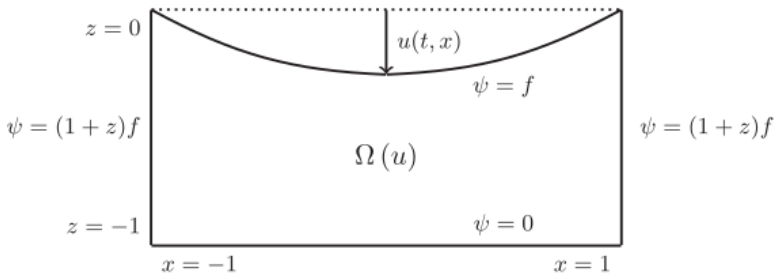

Figure 1: Cross section of a MEMS device.

in the inhomogeneous Dirichlet boundary condition (5), see [12–15], and thus also on the right-hand side of (1).

As the membrane deflects with time the region

$$\Omega(u(t)) = \{(x,z) \in I \times (-1,\infty); -1 < z < u(t,x)\} \tag{6}$$

between the rigid ground plate and the membrane changes with time as well.

Observe that the right-hand side of the evolution equation depends on the partial derivatives of the potential ψ, whence the equations (1) and (4) are strongly coupled. Even more: given the fact that ψ is the solution to the elliptic free boundary value problem (4) and (5), the coupling in (1) is not only nonlinear, but in fact nonlocal as well. Nonetheless, this system is well-posed locally in time. In order to state a precise result, let us introduce the following notation. Given $q \in (2,\infty)$ and $\kappa \in (0,1)$, define the set

$$S_q(\kappa) := \left\{ u \in W^2_{q,D}(I);\ \|u\|_{W^2_{q,D}(I)} < 1/\kappa \ \textit{and}\ -1+\kappa < u(x) \text{ for } x \in I \right\}$$

and

$$W^2_{q,D}(I) := \left\{ u \in W^2_q(I);\ u(\pm 1) = 0 \right\}.$$

Using this notation we may formulate the following result, first established in [10, theorem 3.5 (i)].

Theorem 1 (Local well-posedness)**.** *Let $q \in (2,\infty)$, $\varepsilon > 0$, textand $\lambda > 0$ be given. Assume further that an initial value $u_* \in W^2_{q,D}(I)$ with $u_*(x) > -1$ for $x \in I$, and $f \in C^1([-1,1],\mathbb{R})$ with $\min(f) > 0$ are given. Then there exists a unique maximal solution (u,ψ) to (1-5) on the maximal interval $[0,T)$ of existence in the sense that*

$$u \in C^1\left([0,T), L_q(I)\right) \cap C\left([0,T), W^2_{q,D}(I)\right)$$

satisfies (1-3) with

$$u(t,x) > -1,\ t \in [0,T),\ x \in I$$

and $\psi \in W^2_2(\Omega(u(t)))$ solves (4) and (5) on $\Omega(u(t))$ for each $t \in [0,T)$.

It is the intention of this contribution to compare recent results on qualitative properties of solutions to the above coupled system with those concerning the small-aspect ratio model — its still commonly used reduced counterpart. In this reduction the aspect ratio ε of the device is assumed to be very small, i.e. the problem is considered as if the two plates were locally parallel. Formally, sending ε to zero in (4) leads to the explicit expression

$$\psi(t,x,y) = \frac{1+z}{1+u(t,x)} f(x), \quad t > 0,\ (x,z) \in \Omega(u(t)), \tag{7}$$

for the solution to the simplified electrostatic problem. As a consequence the displacement of the membrane is required to behave according to the small-aspect ratio model

$$u_t - u_{xx} = -\lambda \left(\frac{f(x)}{1+u(t,x)} \right)^2 \qquad t > 0,\ x \in I, \tag{8}$$

$$u(t,\pm 1) = 0, \quad t > 0, \tag{9}$$

$$u(0,x) = u_*(x), \quad x \in I. \tag{10}$$

This simplified semilinear model equation is able to capture several qualitative properties of the coupled system (1)–(5), see [2, 3, 5–8]. However, there are also significant differences observed in the dynamic behavior as we shall see below. More precisely, investigating the right-hand sides of the evolution

equations (1) and (8), respectively, different sign properties of the membrane's displacement become apparent. It is worthwhile to emphasize that this sign property is strongly related to the structure of the chosen permittivity profile.

The simplest permittivity profile — however often used in concrete applications — is $f \equiv 1$. In this case the coupled system involves the evolution equation (1) in the form

$$u_t - u_{xx} = -\lambda \left(\varepsilon^2 \psi_x^2(t,x,z) + \psi_z^2(t,x,z)\right), \ t > 0, \ x \in I.$$

With $\psi(t,x,z) = (1+z)/(1+u(t,x))$ the corresponding small-aspect ratio equation (8) is given by

$$u_t - u_{xx} = -\frac{\lambda}{(1+u)^2}, \quad t > 0, \ x \in I$$

Consequently, given a non-positive initial datum $u_* \leqslant 0$, the parabolic comparison principle implies that both initial boundary value problems possess non-positive solutions. In other words, in both settings a constant permittivity profile causes non-positive initial deflections to evolve towards the ground plate.

Given a spatially varying permittivity profile $f = f(x)$, the situation is fairly different. In this regime the evolution equation (1) reads

$$u_t - u_{xx} = -\lambda \left(\varepsilon^2 \psi_x^2(t,x,z) + \psi_z^2(t,x,z)\right) + 2\lambda\varepsilon^2 \psi_x(t,x,z) f'(x), \quad t > 0, \ x \in I \tag{11}$$

whereas with $\psi(t,x,z) = f(x)(1+z)/(1+u(t,x))$ the according small-aspect ratio equation (8) is given by

$$u_t - u_{xx} = -\lambda \left(\frac{f(x)}{1+u}\right)^2, \quad t > 0, \ x \in I$$

Consulting again the parabolic comparison principle, it turns out that the solution to the small- aspect ratio model is still non-positive for all times $t > 0$ and all $x \in I$. Due to the additional term $2\lambda\varepsilon^2\psi_x(t,x,z)f'(x)$ on the right-hand side of (11) non-positivity of u can no longer be expected as a general feature of the equation[3]. In fact it is the primary concern of this note to provide numerical evidence for the existence of permittivity profiles $f = f(x)$ leading to solutions of (1-3) which possess positive function values; some presumably even never become negative!

We close this introduction by presenting the following convergence result for the limit $\varepsilon \to 0$

Theorem 2 (Small aspect-ratio limit, [11]). *] Let $\lambda > 0$, $q \in (2,\infty)$, $\kappa \in (0,1)$, $f \in C^1([-1,1],(0,\infty))$, and let $u_* \in S_q(\kappa)$ with $u_* < 1 + C$ for $x \in I$. For $\varepsilon > 0$ let $(u_\varepsilon, \psi_{xx}\varepsilon)$ be the unique solution to (1-5), on the maximal interval $[0,T)$ of existence. Then there are $\tau > 0$, $\varepsilon_* \in (0,1)$, and $\kappa_* \in (0,1)$, depending only on q and κ, such that $T \geqslant \tau$ and $u_*(t) \in S_q(\kappa_*)$ for all $t \in [0,\tau]$ and for all $\varepsilon \in (0,\varepsilon_*)$. Moreover, the small aspect-ratio problem (8-10) has a unique solution*

$$u_0 \in C^1([0,\tau], L_q(I)) \cap C\left([0,\tau], W^2_{q,D}(I)\right)$$

satisfying $u_0(t) \in S_q(\kappa_*)$ for all $t \in [0,\tau]$ and such that the convergences

$$u_\varepsilon \longrightarrow u_0 \quad in \quad C^{1-\theta}\left([0,\tau], W^{2\theta}_{q,D}(I)\right), \quad \theta \in (0,1),$$

and

$$\psi_\varepsilon(t)\chi_{\Omega(u_\varepsilon)(t)} \longrightarrow \psi_0(t)\chi_{\Omega(u_0)(t)} \quad in \quad L_2(I \times (-1,0)), \quad t \in [0,\tau], \tag{12}$$

hold true as $\varepsilon \to 0$. Here ψ_0 is the potential given in (7). Furthermore, there exists a $\Lambda(\kappa) > 0$ such that the above results hold true for each $\tau > 0$ provided that $\lambda \in (0,\Lambda(\kappa))$.

Combing this convergence result with the numerical experiments provided in the subsequent section it becomes evident that model reduction of coupled MEMS systems by considering the small-aspect ratio model demands caution: there are phenomena which may be observed just in the limiting case $\varepsilon \to 0$, whereas even for very small $\varepsilon > 0$ a completely different behaviour may occur. In addition, it is worthwhile to mention that there are applications where the device's aspect ratio is such that the assumption $\varepsilon \simeq 0$ is not reasonable or at least debatable.

2 Numerical results

As already mentioned the reduced small-aspect ratio model (8-10) is able to capture various qualitative properties of the coupled system (1-5), such as evenness with respect to $x \in I$, the existence of a pull-in voltage λ^*, as well as global existence for small values $\lambda < \lambda_*$ of the applied voltage. In the case

[3] Sufficient conditions to ensure non-negativity of solutions have been presented recently in [10].

of a constant permittivity profile even the sign property (of u) is preserved when reducing the model to the small-aspect ratio regime. However, this section serves the purpose of specifying permittivity profiles $f = f(x)$ leading even for fairly small $\varepsilon > 0$ to positive deformations u of the membrane. In contrast to that positivity of solutions u_0 to the small aspect-ratio model is impossible as a consequence of the maximum principle[4]. A numerical scheme is set up by first transforming the elliptic boundary value problem for the electrostatic potential to the fixed rectangle $\Omega = I \times (-1, 0)$ by means of the diffeomorphism

$$T_u(x, z) := \left(x, \frac{1+z}{1+u(x)}\right), \quad (x, z) \in \Omega(u)$$

The resulting nonlinear elliptic boundary value problem is then approximated by Galerkin's method using bilinear finite elements on an equidistant rectangular grid of size 40×80. The nonlinear evolution for the membrane's displacement is approximated by the Crank–Nicolson method on an equidistant decomposition of the time interval [0,1] with an increment of 1/100. The resulting system of nonlinear equations is solved via Newton's method. Furthermore, the numerical integration is realized by a Gauß–Legendre quadrature with two Gauß points in both coordinate directions. The implementation is performed in MATLAB[5].

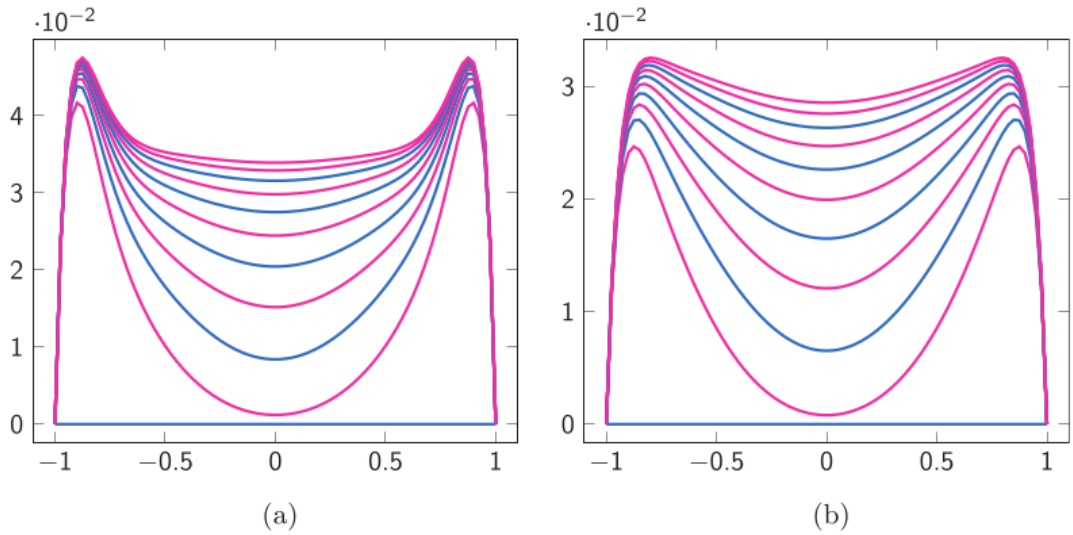

Figure 2: Membrane's deflection u of the coupled system for $f(x) = x^8 + 0.1$ with $u_* \equiv 0$, $\lambda = 1$, and $\varepsilon \in \{0.4, 0.6\}$.

Figures 2–4 illustrate for the permittivity profile

$$f(x) := x^8 + 0.1, \quad x \in [-1, 1]$$

the approximate solution to (1–3) with $u_* \equiv 0$ at different time levels for decreasing values of the aspect ratio ε and $\lambda = 1$. More precisely, choosing $T = 1$ and the time increment 1/100, the curves represent the approximate membrane's displacement at every tenth time step, to be read from bottom up.

Figure 2 reveals that for $\varepsilon \in \{0.4, 0.6\}$ the approximate solution instantaneously becomes positive at all interior points $x \in I$ and increases as time passes.

A different behaviour may be observed in figures 3 and 4. Here the aspect ratio takes the values $\varepsilon \in \{0.1, 0.15, 0.2\}$. In the case $\varepsilon = 0.2$ the solution is still increasing in time. Although it develops initially also negative values it finally becomes strictly positive at all interior points, see figure 3(a). In clear contrast to that is the behaviour when the aspect ratio is reduced to the value $\varepsilon = 0.1$. Then the membrane moves monotonically towards the ground plate at all interior points $x \in I$, as illustrated in figure 3(b).

A quite interesting dynamics may be observed for the value $\varepsilon = 0.15$. Emerging from the initial position $u_* \equiv 0$, the magenta curve in figure 4 shows the approximate solution at time $t = 1/100$. The curves of the approximate solutions at all further time levels seem to coincide in the single blue curve, since it represents the solutions at time levels $t = 10/100,\ 20/100,\ 30/100, \ldots$, until the maximal computing time $T = 1$ is reached. That leads to the conjecture that the blue curve in figure 4 might be

[4]Note that in the settings $f = f(u)$ and $f = f(x, u)$ this reasoning is no longer possible since in these cases the evolution equation's right-hand sides are more involved (see [4, 10]).

[5]Version 8.4.0.150421 (R2014b).

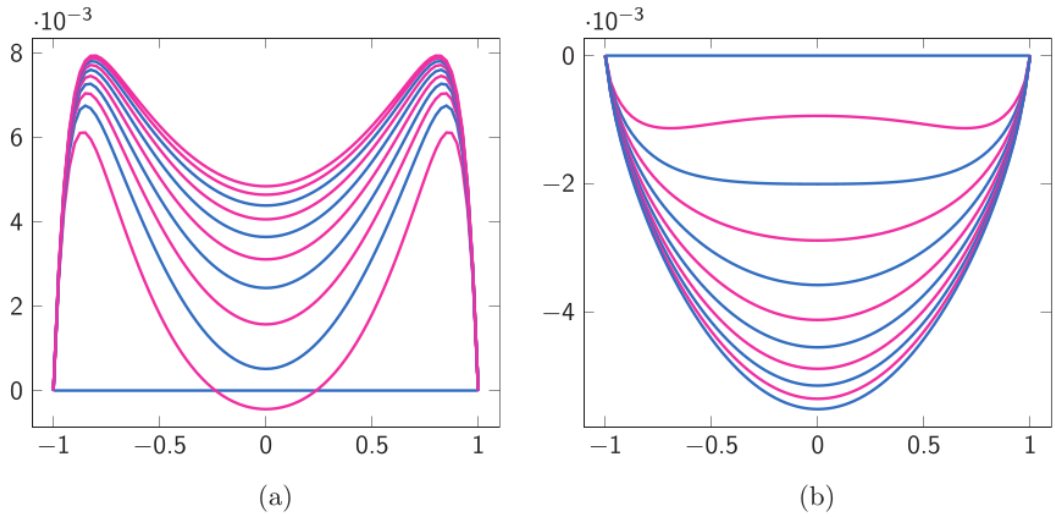

Figure 3: Membrane's deflection u of the coupled system for $f(x) = x^8 + 0.1$ with $u_* \equiv 0$, $\lambda = 1$, and $\varepsilon \in \{0.1, 0.2\}$.

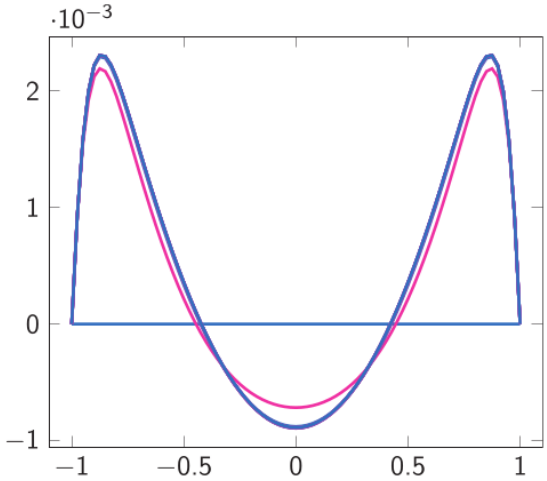

Figure 4: Membrane's deflection u of the coupled system for $f(x) = x^8 + 0.1$ with $u_* \equiv 0$, $\lambda = 1$, and $\varepsilon = 0.15$.

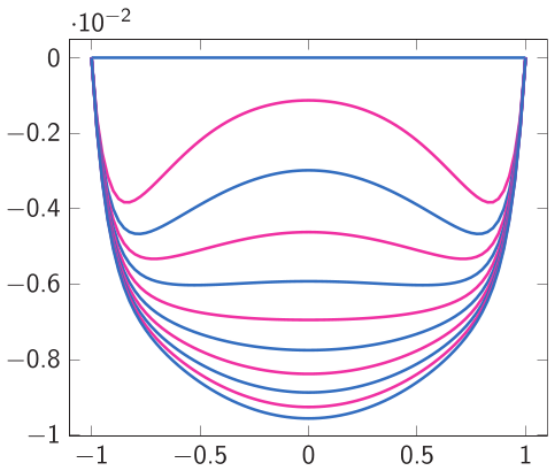

Figure 5: Approximation solution to the small aspect-ratio model with $u_* \equiv 0$ for $f(x) = x^8 + 0.1$ and $\lambda = 1$.

an equilibrium of the evolution in the case of an aspect ratio $\varepsilon = 0.15$ and a value $\lambda = 1$ of the applied voltage.

The above observations for the coupled system with positive values of ε have to be compared with the dynamics of the small-aspect ratio model, see figure 5: in this figure the time evolution of the approximate solution is to be read top down: the deflection of the membrane (emerging from the initial state $u_* \equiv 0$) becomes immediately negative (in all interior points $x \in I$) and seems to decrease monotonically as time passes.

We close our presentation of numerical experiments with the following observation. In figure 6 the approximate solutions of the coupled system with $\varepsilon = 0.85$ and $\lambda = 1$ is depicted. A spike like behaviour near the boundary points $x = \pm 1$ is embedded in the dynamics of sign-changing solutions.

The above numerical experiments may be summarized by the following conjecture and remarks.

Conjecture 1. *Let $u(t, x)$ denote the solution to (1–3) emerging from the initial condition $u_* \equiv 0$. Then we expect the following to be true:*

(i) Given $\varepsilon > 0$, there exist $\lambda > 0$ and smooth positive permittivity profiles $f = f(x)$ such that we have $u(t, x) > 0$ for some $t > 0$ and some $x \in I$.

(ii) There exist $\varepsilon > 0$, $\lambda > 0$ and a smooth positive permittivity profiles $f = f(x)$ such that $u(t, x) > 0$ for all $t \in (0, T)$ and all $x \in I$.

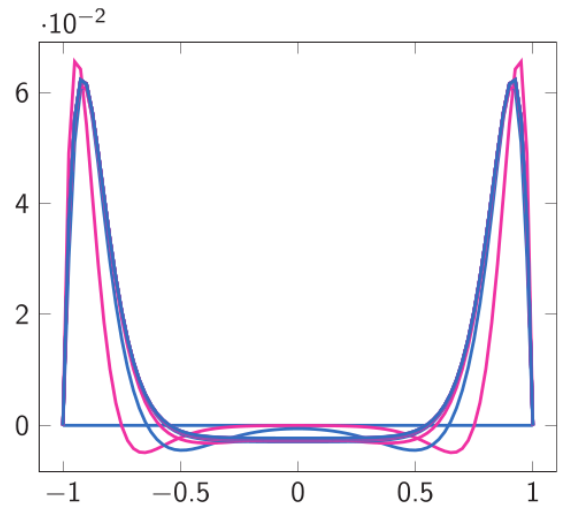

Figure 6: Membrane's deflection u of the coupled system for $f(x) = x^8 + 0.1$ with $u_* \equiv 0$, $\lambda = 1$, and $\varepsilon = 0.85$.

Remark 1. *(i) In view of theorem 2 it is apparent that given a positive permittivity profile $f = f(x)$, there is an $\varepsilon_0 > 0$ such that $u(t,x) \leqslant 0$ on $[0,T) \times [-1,1]$ for all $\varepsilon \in (0,\varepsilon_0)$.*

(ii) In general the maximal existence time $T > 0$ provided in theorem 1 is finite. If $T < \infty$ then either a blow-up of the $W_q^2(I)$-norm of u or a touchdown takes place. More precisely, the singularities are of the form

$$\liminf_{t\to T} \min_{x\in[-1,1]} u(t,x) = -1 \quad \text{or} \quad \limsup_{t\to T} \|u(t,\cdot)\|_{W_q^2(I)} = \infty.$$

If conjecture 1 (ii) is correct then there are $\varepsilon > 0$, $\lambda > 0$, and $f = f(x)$ such that a touchdown is ruled out: either the corresponding solution exists forever or its $W_q^2(I)$-norm blows up in finite time.

(iii) The reported phenomena are not restricted to the profile $f(x) = x^8 + 0.1$. Similar results are observed e.g. for $f(x) = x^{2k} + 0.1$ with $k \in \{1, 2n3, \ldots\}$ and $f(x) = \exp(ax^2)$ with $a \in [1,3]$.

3 A formal derivation of the first variation of the potential energy

The difference in the dynamic behaviour of solutions to the coupled system (1)–(5) and that of solutions to its small-aspect ratio counterpart originates from the structure of the respective right-hand sides. In this section we formally show that steady states of (1)–(5) are critical points of the total potential energy of the system. To make this more clear assume that $u \in C^\infty([-1,1],\mathbb{R})$ satisfies $u(\pm 1) = 0$ and

$$u_{xx} - \lambda\left(\varepsilon^2\psi_x^2(t,x,z) + \psi_z^2(t,x,z) - 2\varepsilon^2\psi_x(t,x,z)f'\right) = 0, \tag{13}$$

where $\psi(x,z)$ solves

$$\varepsilon^2\psi_{xx} + \psi_{zz} = 0, \quad (x,z) \in \Omega(u), \tag{14}$$

$$\psi(x,z) = \frac{1+z}{1+u(x)} f(x), \quad (x,z) \in \partial\Omega(u). \tag{15}$$

We further introduce the linearized stretching energy

$$E_s(u) := \frac{1}{2}\int_{-1}^{1} u_x^2 \mathrm{dx}$$

and the electrostatic energy

$$E_e(u) := \int_{\Omega(u)} \left(\varepsilon^2\psi_x^2(t,x,z) + \psi_z^2(t,x,z)\right) \mathrm{d(x,z)}$$

The total potential energy is then given by $E_p(u) = E_s(u) - \lambda E_e(u)$, where the parameter λ is proportional to the square of the applied voltage. Given a test function $\theta \in C_c^\infty((-1,1))$ we are going to compute the first variation $\delta E_p(u;\theta)$ of $E_p(u)$ in the direction θ, i.e.

$$\delta E_p(u;\theta) = \frac{d}{d\sigma} E_p(u + \sigma\theta)|_{\sigma=0}.$$

To this end, we need to parametrise the domains $\Omega_\sigma = \Omega(u+\sigma\theta)$ induced by the family

$$\{u+\sigma\theta; \sigma \in (-\sigma_0, \sigma_0)\},$$

where $\sigma_0 > 0$ is chosen in such a way that

$$u(x) + \sigma\theta(x) > -1 \quad \text{for all} \quad (x,\sigma) \in [-1,1] \times [-\sigma_0, \sigma_0].$$

We denote by $\psi(\sigma; u)$ the solution to

$$\varepsilon^2 \psi_{xx}(\sigma; u) + \psi_{zz}(\sigma; u) = 0, \quad (x,z) \in \Omega_\sigma, \tag{16}$$

$$\psi(\sigma; u)(x,z) = \frac{1+z}{1+u(x)} f(x), \quad (x,z) \in \partial\Omega_\sigma \tag{17}$$

Furthermore, we introduce the velocity[6]

$$\mathcal{V} := \frac{d}{d\sigma}\psi(\sigma; u)|_{\sigma=0}, \quad (x,z) \in \Omega(u)$$

of the path $\{\psi(\sigma; u); \sigma \in (-\sigma_0, \sigma_0)\}$ at u. Given $(x,z) \in \Omega(u)$, observe now that

$$\varepsilon^2 \psi_{xx}(\sigma; u)\left(x, z + \sigma\theta(x)\frac{1+z}{1+u(x)}\right) + \psi_{zz}(\sigma; u)\left(x, z + \sigma\theta(x)\frac{1+z}{1+u(x)}\right) = 0.$$

Differentiating this equality with respect to σ and sending afterwards σ to zero, we arrive at the following equation:

$$\varepsilon^2 \mathcal{V}_{xx} + \mathcal{V}_{zz} + \theta(x)\frac{1+z}{1+u(x)}\left(\varepsilon^2 \psi_{xxz}(0; u) + \psi_{zzz}(0; u)\right) = 0, \quad (x,z) \in \Omega(u).$$

Invoking (16), we see that

$$\varepsilon^2 \psi_{xxz}(0; u) + \psi_{zzz}(0; u) = 0, \quad (x,z) \in \Omega(u).$$

implying that $\mathcal{V}$ solves

$$\varepsilon^2 \mathcal{V}_{xx} + \mathcal{V}_{zz} = 0, \quad (x,z) \in \Omega(u).$$

In order to identify the boundary condition satisfied by $\mathcal{V}$, we note that (167) may be written as

$$\psi(\sigma; u)\left(x, z + \sigma\theta(x)\frac{1+z}{1+u(x)} = \frac{1+z}{1+u(x)} f(x), \quad (x,z) \in \partial\Omega(u).\right)$$

Again, differentiation of this identity with respect to σ and evaluating the result at $\sigma = 0$ yields

$$\mathcal{V}(x,z) = -\theta(x)\frac{1+z}{1+u(x)}\psi_z(0; u)(x,z), \quad (x,z) \in \partial\Omega(u).$$

Summarizing the above observations, the function $\mathcal{V}$ complies with the elliptic boundary value problem

$$\varepsilon^2 \mathcal{V}_{xx} + \mathcal{V}_{zz} = 0, \quad (x,z) \in \Omega(u), \tag{18}$$

$$\mathcal{V}(x,z) = -\theta(x)\frac{1+z}{1+u(x)}\psi_z(0; u)(x,z), \quad (x,z) \in \partial\Omega(u). \tag{19}$$

We now use the transport theorem, see [1, theorem XII.2.11], to obtain

$$\delta E_e(u;\theta) = -\int_{\Omega(u)} \left[2\varepsilon^2 \psi_x(0; u)\mathcal{V}_x + 2\psi_z(0; u)\mathcal{V}_z + \operatorname{div}\left((\varepsilon^2 \psi_x^2(0; u) + \psi_z^2(0; u))\phi'_\sigma(0)\right)\right] \mathrm{d(x,z)}$$

where $\phi_\sigma(\sigma)$ is a diffeomorphism which maps $\Omega(u) = \Omega_0$ onto $\Omega_0\sigma$, e.g.

$$\phi_\sigma(\sigma)(x,z) := \left(x, z + \sigma\theta(x)\frac{1+z}{1+u(x)}\right), \quad (x,y) \in \Omega(u)$$

In order to simplify our notation we set

$$\psi_x := \psi_x(0; u) \quad \text{and} \quad \psi_z := \psi_z(0; u).$$

[6] Note that in fact $\mathcal{V}$ is a function of the variables x and z in the sense that $\mathcal{V}(x,z) := \frac{d}{d\sigma}\psi(\sigma; u)|_{\sigma=0}(x,z)$.

Observing (16), we notice that

$$\operatorname{div}\left(\mathcal{V}(\varepsilon^2\psi_x,\psi_z)\right)=\varepsilon^2\mathcal{V}_x\psi_x+\mathcal{V}_z\psi_z.$$

Thus we find that

$$\delta E_e(u;\theta)=-\int_{\Omega(u)}\left[2\operatorname{div}\left(\mathcal{V}(\varepsilon^2\psi_x,\psi_z)\right)+\operatorname{div}\left((\varepsilon^2\psi_x^2+\psi_z^2)\phi'_\sigma(0)\right)\right]\mathrm{d(x,z)} \tag{20}$$

It follows from (19) that $\mathcal{V}$ vanishes on the ground plate and on the lateral boundaries of $\Omega(u)$. The very same is true for $\phi'_\sigma(0)$, since

$$\phi_\sigma\sigma'(0)(x,z):=\left(0,\theta(x)\frac{1+z}{1+u(x)}\right),\quad (x,z)\in\Omega(u).$$

Applying the divergence theorem to (20) thus yields

$$\delta E_e(u;\theta)=-\int_{-1}^{1}[2\mathcal{V}(x,u(x))\left(-\varepsilon^2\psi_x(x,u(x))u_x(x)+\psi_z(x,u(x))\right)$$
$$+\theta(x)\left(\varepsilon^2\psi_x^2(x,u(x))+\psi_z^2(x,u(x))\right)]\mathrm{dx} \tag{21}$$

Using the only nontrivial boundary condition for $\mathcal{V}$ we find that

$$\mathcal{V}(x,u(x))\left(-\varepsilon^2\psi_x(x,u(x))u_x(x)+\psi_z(x,u(x))\right)=\theta(x)\left(\varepsilon^2\psi_x(x,u(x))\psi_z(xnu(x))u_x(x)-\psi_z^2(x,u(x))\right)$$

for all $x\in I$. Differentiating furthermore the boundary condition $\psi(x,u(x))=f(x)$ with respect to x, we get

$$\psi_z(x,u(x))u_x(x)=f('x)-\psi_x(x,u(x)),\quad x\in I$$

Fusing the last two identities we may conclude that

$$2\mathcal{V}(x,u(x))(-\varepsilon^2\psi_x(x,u(x))+\psi_z(x,u(x)))$$
$$=2\theta(x)\left(\varepsilon^2\psi_x(x,u(x))f'(x)-\varepsilon^2\psi_x^2(x,u(x))-\psi_z^2(x,u(x))\right). \tag{22}$$

Combining (21) with (22) we arrive at

$$\delta E_e(u;\theta)=-\int_{-1}^{1}\theta(x)\left[-2\varepsilon^2\psi_x(x,u(x))f'(x)+\varepsilon^2\psi_x^2(x,u(x))+\psi_z^2(x,u(x))\right]\mathrm{dx}$$

It remains to calculate the first variation of the stretching energy:

$$\delta E_s(u;\theta)=\int_{-1}^{1}u_x(x)\theta_x(x)\mathrm{dx}=-\int_{-1}^{1}u_{xx}(x)\theta(x)\mathrm{dx}.$$

Merging the last two equations we arrive at

$$\delta E_p(u;\theta)=-\int_{-1}^{1}\theta(x)\left[u_{xx}-\lambda\left(\varepsilon^2\psi_x^2(x,u(x))+\psi_z^2(x,u(x))+2\varepsilon^2\psi_x(x,u(x))f'(x)\right)\right]\mathrm{dx}$$

showing that $\delta E_p(u;\theta)=0$ thanks to (13).

A combination of the above considerations leads to the following statement.

Observation 1. *Stationary solutions to (1–3) are critical points of the potential energy $E_p(u)$.*

As mentioned earlier, the above reasoning is formal since we do not specify the regularity of $\psi(\sigma;u)$ neither with respect to the parameter σ not with respect to the variables $(x,z)\in\Omega_\sigma$. Following however the linear of [9, proposition 2.2], equation (23) may be justified rigorously.

There is a further interpretation of (23). Indeed, given $u\in W^2_{2,D}(I)$, let

$$\nabla E_p(u):=-u_{xx}+\lambda\left(\varepsilon^2\psi_x^2(\cdot,u)+\psi_z^2(\cdot,u)\right)-2\varepsilon^2\psi_x(\cdot,u)f'(x),$$

where $\psi(x,z)$ complies with (14) and (15). Assume further that $\nabla E_p(u)\in L_2(I)$, which may be realised if u possesses enough spatial regularity[7]. Then we conclude from (23) that

$$(\nabla E_p(u),\theta)_{L_2(I)}=\delta E_p(u;\theta)\quad \textit{for all } \theta\in C_c^\infty(I).$$

Thus $\nabla E_p(u)$ may be considered as a generalized gradient of E_p at u in $L_2(I)$ and (11) formally becomes

$$u_t=-\nabla E_p(u(t)),\quad t>0,$$

i.e. (11) represents the gradient flow in $L_2(I)$ induced by E_p.

[7] In fact it follows from [3, relation (39)] that $u\in W^2_q(I)$ with $q>2$ is sufficient.

Acknowledgment

The authors are grateful to G Starke for fruitful discussions on the implementation of the numerical scheme. Furthermore, discussions on various topics on MEMS with P Laurençot and C Walker are acknowledged by JE. Moreover, the authors are thankful to the referees and the editors of Nonlinearity for their helpful remarks and suggestions. Finally, this research project has been financially supported by the DFG IRTG 1627.

References

1. Amann H and Escher J 2008 Analysis III (Basel: Birkhäuser)
2. Brubaker N D and Pelesko J A 2011 Non-linear effects on canonical MEMS models Euro. J. Appl. Math. 22 455–70
3. Escher J, Laurençot P and Walker C 2014 A parabolic free boundary problem modeling electrostatic MEMS Arch. Ration. Mech. Anal. 211 389–417
4. Escher J and Lienstromberg C 2016 A qualitative analysis of solutions to microelectromechanical systems with curvature and nonlinear permittivity profiles Commun. PDE 41 134–49
5. Esposito P, Ghoussoub N and Guo Y 2010 Mathematical Analysis of Partial Differential Equations Modeling Electrostatic MEMS (Courant Lecture Notes in Mathematics vol 20) (New York: Courant Institute of Mathematical Sciences)
6. Ghoussoub N and Guo Y 2007 On the partial differential equations of electrostatic MEMS devices: Stationary case SIAM J. Math. Anal. 38 1423–49
7. Guo J-S and Souplet P 2015 No touchdown at zero points of the permittivity profile for the MEMS problem SIAM J. Math. Anal. 47 614–25
8. Guo Y, Pan Z and Ward M J 2005 Touchdown and pull-in voltage behavior of a MEMS device with varying dielectric properties SIAM J. Appl. Math. 66 309–38
9. Laurençot P and Walker C 2014 A free boundary problem modeling electrostatic MEMS: I. Linear bending effects Math. Ann. 360 307–49
10. Lienstromberg C 2016 On qualitative properties of solutions to microelectromechanical systems with general permittivity Mon.hefte Math. 179 581–602
11. Lienstromberg C 2015 A free boundary value problem modelling microelectromechanical systems with general permittivity Nonlinear Anal.: RWA 25 190–218
12. Lindsay A E and Ward M J 2008 Asymptotics of some nonlinear eigenvalue problems for a MEMS capacitor. I. Fold point asymptotics Methods Appl. Anal. 15 297–325
13. Pelesko J A 2002 Mathematical modeling of electrostatic MEMS with tailored dielectric properties SIAM J. Appl. Math. 62 888–908
14. Pelesko J A and Bernstein D H 2003 Modeling MEMS and NEMS (Boca Raton, FL: Chapman & Hall)
15. Pelesko J A and Triolo A A 2001 Nonlocal problems in MEMS device control J. Eng. Math. 41 345–66